inorganics

MDPI

Article

Computational Structures and SAPT Interaction Energies of HXeSH···H_2Y (Y=O or S) Complexes

Janusz Cukras [1,*], Grzegorz Skóra [2], Joanna Jankowska [1] and Jan Lundell [3,*]

1 Department of Chemistry, University of Warsaw, Ul. Ludwika Pasteura 1, 02-093 Warsaw, Poland; jjankowska@chem.uw.edu.pl
2 Department of Physics, University of Warsaw, Ul. Ludwika Pasteura 5, 02-093 Warsaw, Poland; gzsa@posteo.eu
3 Department of Chemistry, University of Jyvaskyla, P.O. Box 35, 40014 Jyvaskyla, Finland
* Correspondence: januszc@chem.uw.edu.pl (J.C.); jan.c.lundell@jyu.fi (J.L.); Tel.: +358-40-744-5270 (J.L.)

Received: 14 August 2018; Accepted: 11 September 2018; Published: 19 September 2018

Abstract: Ab initio calculations of the structures, vibrational spectra and supermolecular and symmetry-adapted perturbation theory (SAPT) interaction energies of the HXeOH and HXeSH complexes with H_2O and H_2S molecules are presented. Two minima already reported in the literature were reproduced and ten new ones were found together with some transition states. All complexes show blue shift in Xe–H stretching mode upon complexation. The computed spectra suggest that it should be possible to detect and distinguish the complexes experimentally. The structures where H_2O or H_2S is the proton-donor were found to be the most stable for all complex compositions. The SAPT analysis shows significant differences between the complexes with H_2O and H_2S indicating much larger dispersion and exchange contributions in the complexes with H_2S.

Keywords: Ab initio; SAPT; interaction; complex; noble gas; non-covalent; hydrogen bond

1. Introduction

Hydrogen bonding represents one of the distinctive non-covalent interactions playing an important role in many chemical and biological processes, as well as crystal engineering [1,2]. Hydrogen bonded complexes of water have a significant influence on atmospheric chemistry and are considered to contribute to chemistry of interstellar media and planetary atmospheres [3–5]. Since water is the most important solvent in nature and water vapor is abundant in the atmosphere, it is essential to consider chemical entities and processes when they are influenced by one or more water molecules. Owing to the small size and large dipole moment, water molecule is an efficient source of hydrogen bonds to direct chemical processes, as well as to present a chemical surrounding allowing new chemistry to take place.

Recently, the first experimental evidence for the reactivity of Xe with water ice at conditions found in the interior of giant planets was reported [6]. The study made a connection between noble gas compounds with reactivity of water suggesting that HXeOH and HXeOXeH could be involved in the formation of the Xe-insertion crystal structure $Xe_4O_{12}H_{12}$ identified in high pressure and temperature conditions typical for the interiors of Uranus and Neptune. Both HXeOH [7] and HXeOHXeH [8] belong to the novel group of noble gas compounds, which up-to-now have been prepared in laboratory conditions [9–11]. These neutral molecules of the type HNgY, where Ng is a noble gas atom Ar, Kr or Xe (no such molecules have been experimentally observed for He, Ne or Rn) and Y is an electronegative atom, are characteristically highly ionic but metastable in nature and possess very large dipole moments.

On the other hand, these molecules are very sensitive to their closest chemical neighborhood [12], which is evidenced by strong shifts of their fingerprint Ng–H stretching vibration. For example, the HXeBr···HBr complex in a xenon matrix exhibits large shifts of +150 cm^{-1} from that of the corresponding monomer [13]. There are also examples of the weaker complexes with relatively small shifts, such as the HXeBr···N_2 (+11.5 and +16 cm^{-1}) and HXeCCH···HCCH (from +19 to +28 cm^{-1}) complexes studied in a xenon matrix [14,15].

The number of computational works on complexes of Xe-containing noble-gas hydrides is substantial (e.g., see [16–23]). We investigated hydrogen-bonded complexes of HXeOH [7] and HXeSH [24] formed with their precursor molecules H_2O and H_2S. Quantum chemical calculations and symmetry-adapted perturbation theory were used to study the possible structures of HXeOH-H_2O, HXeOH-H_2S, HXeSH-H_2O and HXeSH-H_2S complexes, the vibrational properties and the characteristics of the origin of the non-covalent interactions. In the case of HXeOH-H_2O complex, several experimental and computational studies exist [12,25–29]. These studies characterized the 1:1 hydrogen-bonded complex thoroughly, and indicated moderate hydrogen bond between the complex subunits. The computational investigations by Nemukhin et al. [25] also demonstrated that hydrogen-bonded cluster involving more than one water molecule decrease the stability of HXeOH, a property that seems to be common for all the noble-gas containing molecules in the presence of increasing number of water molecules [29]. Up-to-date, there appear to be no studies on HXeOH-H_2S, HXeSH-H_2O or HXeSH-H_2S, which could shed light on the similarities and differences of the oxygen- and sulfur-containing complexes and their properties to aid possible future experimental endeavors to prepare and identify such complexes.

2. Computational Details

2.1. Potential Energy Surface Analysis

The studied complexes are sensitive to the treatment method so the chosen methodology is a necessary compromise between computational cost and the requirements of a particular system. The geometry optimization was performed using the Second Order Møller-Plesset Perturbation Theory. We employed the Dunning-type singly augmented aug-cc-pVDZ basis set for the hydrogen, oxygen and sulfur atoms, whereas the xenon atom was assigned the aug-cc-pVDZ-PP basis set comprising Effective Core Potentials (ECP), which allows inclusion of the scalar relativistic effect. This basis set is denoted as aug-cc-pVDZ(-PP).

The obtained structures were optimized starting from many different hypothetical structures set by hand and using the "tight" convergence criteria except for the ε structures, in which case the "very tight" criteria was used. All further calculations, the normal mode analysis, the supermolecular interaction energies with different methods and the SAPT interaction energies were calculated for the structures obtained in this way, i.e., at the MP2/aug-cc-pVDZ(-PP) level of theory. Supporting information to that presented here, is presented in Supplementary Materials as Figures S1–S4 and Tables S1–S22.

Vibrational analysis was done for all stationary points to confirm their nature as a local minimum or a transition state. All found first-order saddle points are also reported in the Supplementary Materials (Figure S4, Tables S17–S22). Anharmonic vibrational analysis was additionally performed for the minima to facilitate the comparison with experimental data. The anharmonic calculations employed the Barone approach [30,31]. Geometry optimization and vibrational analysis were done using Gaussian 09 program [32].

2.2. Supermolecular Interaction Energy

The intermolecular interaction energies of the binary clusters E_{int}^{AB} were calculated using the standard approach, i.e., as the difference of the total energy of the supermolecular complex E_{tot}^{AB}

comprising interacting molecular constituents A and B and the separate energies of the constituents E_{tot}^{A} and E_{tot}^{B}:

$$E_{int}^{AB} = E_{tot}^{AB} - \left(E_{tot}^{A} - E_{tot}^{B}\right) \quad (1)$$

The Basis Set Superposition Error (BSSE) was taken into account using the geometry and the basis set of the entire complex when calculating the values of each term in Equation (1). The deformation energy, which reflects the change in energy originating from the deformation of the constituent molecules upon the formation of the complex, was not included in our analysis.

To evaluate whether the chosen basis set was good for the description of the intermolecular interaction energy (i.e., whether it is close to saturation). we performed additional calculations including midbond functions placed in the middle of the two closest interacting atoms. We chose three *s* and *p* functions with exponents 0.9, 0.3 and 0.1; two *d* functions with exponents 0.6 and 0.2; and one *f* and one *g* function with exponents of 0.3 each.

2.3. Symmetry-Adapted Perturbation Theory (SAPT) Interaction Energy Analysis

To establish the physical nature of the intermolecular interaction in the studied binary complexes, we employed the Symmetry-Adapted Perturbation-Theory approach [33,34]. We refrained to a set of early terms as typically they reflect the nature of the interaction substantially correct. At this level, the corrections taken into account are as follows:

$$E_{int}^{SAPT0} = E_{elst}^{(10)} + E_{exch}^{(10)} + E_{ind,r}^{(20)} + E_{exch-ind,r}^{(20)} + E_{disp}^{(20)} + E_{exch-disp}^{(20)} + \delta E_{int,resp}^{HF} \quad (2)$$

we simplify the notation to facilitate the discussion:

$$E_{elst} = E_{elst}^{(10)} \quad (3)$$

$$E_{exch} = E_{exch}^{(10)} \quad (4)$$

$$E_{ind} = E_{ind,resp}^{(20)} + E_{exch-ind,resp}^{(20)} \quad (5)$$

$$E_{disp} = E_{disp}^{(20)} + E_{exch-disp}^{(20)} \quad (6)$$

$$E_{int}^{SAPT0} = E_{elst} + E_{exch} + E_{ind} + E_{disp} \quad (7)$$

Note that we omit the $\delta E_{int,resp}^{HF}$ term because its use is questionable for the studied complexes, which is discussed below.

The SAPT calculations were carried out using MOLPRO code [35]. Data processing and visualization were done using iPython [36], SciPy [37] and Matplotlib [38] packages.

3. Results and Discussion

3.1. Structures of the Complexes

All optimized equilibrium structures of HXeOH/SH···H_2O/S complexes are shown in Figure 1. The obtained structures can be grouped by the type of the molecule with which the noble-gas molecule forms a complex. There are two structures of the complex of the noble gas molecule with H_2O and four structures when H_2S is involved. The complexes differ from each other with the structure and composition. We have introduced a simple notation to refer to the complexes following the previous study of Cukras and Sadlej [27]. The structures are named with Greek alphabet letters, α, β, γ and ε, and the composition by an indication whether the noble gas molecule contains sulfur or oxygen and whether the accompanying molecule contains sulfur or oxygen, in that order. For example, α-OS indicates that the geometry is of the α type and that the noble gas compound contains oxygen and it forms complex with H_2S. The complex geometries are presented as structural coordinates in

Supplementary Materials (Tables S5–S22). Here, the complex structures are described on a qualitative level as the detailed bond distances and bond angles can be extracted from the structural coordinates.

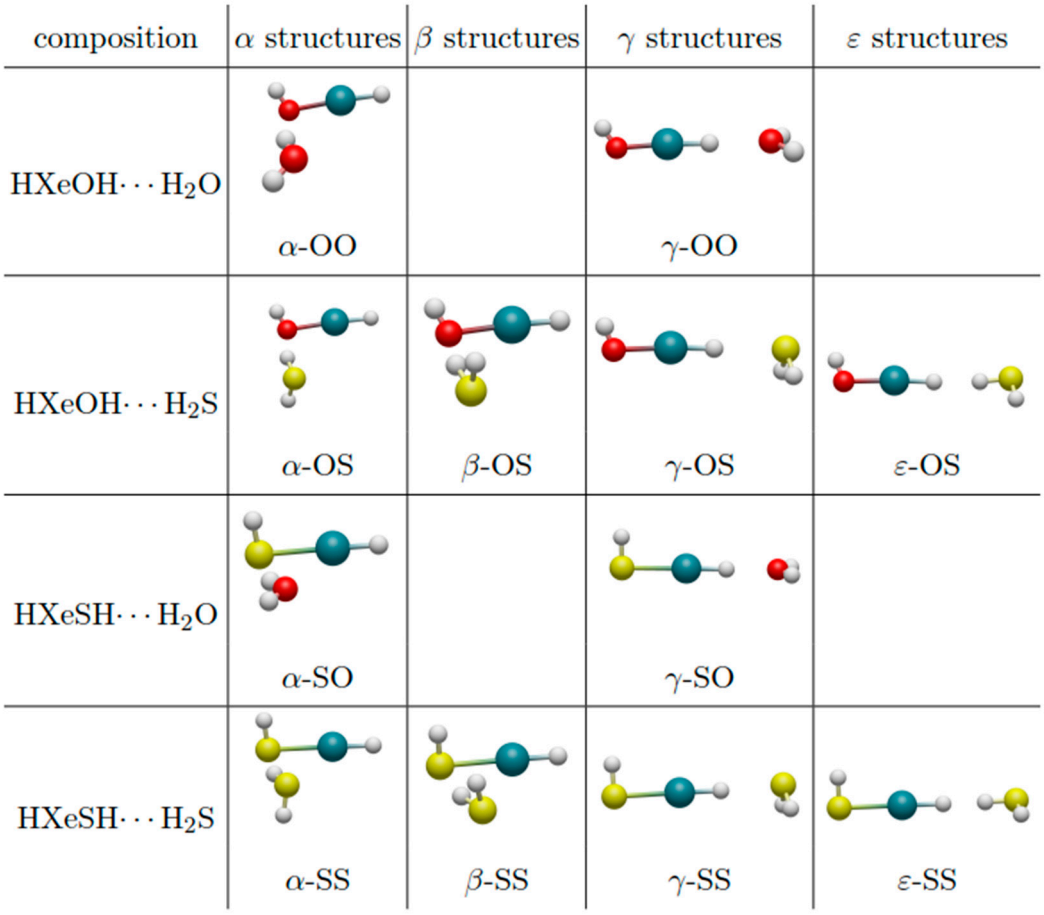

Figure 1. The calculated structures of the complexes of HXeOH and HXeSH with H_2O and H_2S. The atoms of hydrogen, oxygen, sulfur and xenon are marked with white, red, yellow and blue, respectively.

3.1.1. HXeOH/SH Complexes with H_2O

For HXeOH-H_2O complex, two local minima were identified by the MP2/aug-cc-pVDZ(-PP) calculations. The α-OO structure, where water molecule acts as proton donor to the oxygen of the OH group of HXeOH, is the global minimum structure for the complex. This is also the structure identified in low-temperature xenon matrix [25]. The higher energy form γ-OO is a linear structure where the Xe–H tail of HXeOH acts as a proton donor to oxygen of the water molecule. The water molecule hydrogens are slightly tilted out from the plane of the hydrogen bond in analogy to water dimer equilibrium structure. Both structures are in accordance with previous studies on the HXeOH-H2O complex [25–27,29,39]. However, discrepancy exists between the current study and previous computational study. Here, calculations at the MP2/aug-cc-pVDZ(-PP) level could not repeat the structure denoted as δ-OO in reference [27]. This structure shows water molecule as a proton acceptor and the OH tail of HXeOH as proton donor in a hydrogen-bonded complex. Here, the structure was looked for besides MP2 calculations also by Counterpoise corrected MP2 optimization and CCSD(T) optimizations. In all our computational cases, the literature-based structure collapsed into the most stable structure of α-OO. This discrepancy can be traced back to the different basis sets used in the studies, as well as different version of computer codes used. In fact, the only study up to date to report this structure is in ref. [27]. To resolve the existence of the hydrogen-bonded complex formed by the OH tail of HXeOH (or HXeSH), more extensive studies on the basis set

performance were performed. This is, however, outside the current study as this study was more focused on the mixed oxygen/sulfur complexes to warrant the search for such complexes, for example in low-temperature matrix experiments.

The complexes formed between HXeSH and H_2O follow the trend set by the HXeOH-H_2O complex. Two stable structures, i.e., α-SO and γ-SO, were identified, and again the δ-SO structure as a starting point for optimization collapsed to the most stable α-SO structure. The major difference between HXeOH and HXeSH as a proton acceptor subunit in α-structure is the tilt of H_2S towards the xenon atom in the Xe–S···O plane in α-SO compared to water molecule in the Xe–O···O plane in α-OO.

3.1.2. HXeOH/SH Complexes with H_2S

The noble-gas molecule complexes with the H_2S molecule are predicted to have a double amount of stable structures compared to the complexes involving water molecule. The HXeOH/SH···H_2S complexes exhibit four different complex structures, where the α- and γ-structures appear similar to the case of water molecule. The β-OS and β-SS structures are a local minimum structure, where the trans-conformation appearing in the water complexes is twisted into a cis-like orientation of the H_2S molecule, i.e. the OH tail and the non-bonded SH tail are pointing towards the same direction (see Figure 1). In the β-structures, the noble gas molecule is still a proton acceptor similar to the α-structures involving a complex with water molecule. The second new minimum structure appearing for the H_2S complexes is denoted as ε-type complexes. Both structures exhibit a dihydrogen bond (DHB), where the Xe–H tail interacts with the SH-tail of H_2S. These structures are similar to the dihydrogen bonded complex reported previously for HXeH···H_2O complex [24,40]. Typically, the dihydrogen bond distances have been determined to be in the range 1.7–2.2 Å [41–43]. Here, the intermolecular bond distances for ε-OS and ε-SS are 2.0049 and 1.8307 Å, respectively. These values are slightly longer than the 1.7111 Å reported for HXeH-H_2O complex [40], but still along the general trend of reported studies on dihydrogen bonds.

The computed Mulliken charges for the HXeOH/SH monomers and their H_2S complexes are shown in Table 1. The computed values indicate that upon complexation the ionic character $(OH)^-(Xe–H)^+$ of the HXeOH/SH molecules increases compared with the isolated monomers. The increased partial charge separation is also the reason the intermolecular distance in HSXeH···HSH is shorter than the one in the HOXeH···HSH complex. This behavior upon dihydrogen bonding is analog to the HXeH-H_2O case, where the existence of hydrogen-bonded interaction was analyzed based on the Electron Localization Function (ELF), and found to be largely electrostatic in origin [24].

Table 1. MP2/aug-cc-pVDZ(-PP) computed Mulliken charges for the HXeOH/HXeSH) molecules and their dihydrogen bonded complexes with H_2S.

Atom	HXeOH	ε-OS	HXeSH	ε-SS
H	0.032	0.084	−0.117	0.044
O/S	−0.622	−0.785	−0.519	−0.601
Xe	0.622	0.874	0.611	0.932
H(bonded to Xe)	−0.032	−0.198	−0.025	−0.360
H(DHB)	-	−0.021	-	−0.046
S	-	−0.045	-	−0.054
H	-	0.091	-	0.085

3.2. Vibrational Frequencies

The computed vibrational spectra for the monomers and the most stable complexes are presented in Table 2. Both harmonic and anharmonic spectra are presented along with vibrational shifts according to anharmonic calculations and infrared intensities according to harmonic calculations.

3.2.1. Monomer Spectra

The vibrational spectra computed for H_2O and H_2S correspond reasonably well to the gas phase vibrational data presented by Shimanouchi [44]. For H_2O, the computed anharmonic frequencies are 3747 (ν_{as} (OH)), 3622 (ν_s (OH) and 1575 cm^{-1} (δHOH)) when the corresponding gas phase values are 3756, 3657 and 1595 cm^{-1}, respectively. In the case of H_2S, the computations yield 2682 (ν_{as} (SH)), 2658 (ν_s (SH) and 1166 cm^{-1} (δHSH)), and the corresponding gas phase values are 2626, 2614 and 1183 cm^{-1}, respectively. The computational IR intensities for these three modes appear very small based on the MP2/aug-cc-PVDZ(-PP) calculations yielding only 0.01, 0.1 and 0.6 km·mol^{-1}, respectively. This is the reason these intensities appear as null for all the modes in Table 2.

For HXeOH and HXeSH, the comparison can be made with the IR data obtained in low temperature xenon matrices, where only the Xe–O/S stretching mode has been observed for these molecules. Both stretching modes are computed to be very strong and therefore they appear as convenient fingerprints for the noble gas molecules. The ν Xe–H stretching mode has been reported to lie at 1577.7 and 1118.6 cm^{-1} for HXeOH and HXeSH, respectively. Both Xe–H stretching frequencies are computed here to be too high compared to the experimental values, i.e. +145 cm^{-1} for HXeOH and +256 cm^{-1} for HXeSH. This is due to the electron correlation and basis set effects, as demonstrated earlier by Lundell et al. [45] for several noble gas molecules. Accordingly, combining CCSD(T) harmonic calculations with MP2 level anharmonic corrections appears to give reasonable positions for the Xe–H stretching modes in comparison with experimental (matrix isolation) data.

3.2.2. Complex Spectra

When the noble gas compound HXeOH/SH is complexed, the most stable structures of α-type breaks the symmetry of the H_2O or H_2S subunits. Accordingly, there are two modes representing the hydrogen-bonded O/S–H stretching mode and the non-hydrogen bonded O/S–H stretching mode. The latter shows a modest downward shift in vibrational frequency compared to the isolated molecule, whereas the hydrogen bonded O/S–H stretch is strongly red-shifted and notably gains intensity. In the HXeOH and HXeSH complexes, the hydrogen-bonded OH stretching mode is shifted -383 and -235 cm^{-1}, respectively, compared to the symmetric stretching mode in isolated water molecule. In the case of H_2S, the shifts are computed to be -382 and -176 cm^{-1} for the α-OS and α-SS complexes, respectively. Similarly, large red-shifts are also computed to the related β-complexes involving H_2S subunit. Based on these findings, it is surprising that no experimental reports of such strong OH stretching modes in HXeOH···H_2O complex have been reported thus far, even though the complex has been identified in xenon matrix [25].

Table 2. The harmonic and anharmonic fundamental mode wavenumbers (in cm^{-1}) and their infrared intensities (in $km \cdot mol^{-1}$) of the most stable complexes compared with their isolated subunits. All calculations were performed on the MP2/aug-cc-pVDZ(-PP) level of theory.

ν_{harm}	ν_{anh}	I	ν_{harm}	ν_{anh}	$\Delta\nu_{anh}$ [1]	I	ν_{harm}	ν_{anh}	$\Delta\nu_{anh}$ [1]	I	ν_{harm}	ν_{anh}	$\Delta\nu_{anh}$ [1]	I
	H_2O			α-OO				α-OS				β-OS		
3938	3747	67	3894	3708	−39	55	-	-	-	-	-	-	-	-
3803	3622	4	3401	3239	−383	679	-	-	-	-	-	-	-	-
1622	1575	67	1663	1605	30	57	-	-	-	-	-	-	-	-
	HXeOH													
3766	3610	55	3778	3600	−10	55	3767	3591	−19	60	3770	3595	−15	62
1809	1722	1087	1917	1812	90	826	1888	1782	60	894	1888	1781	59	891
824	818	6	779	732	−86	33	789	773	−45	1	787	768	−50	1
633	630	0	617	599	−31	1	630	581	−49	26	626	593	−37	13
586	597	3	564	554	−43	5	610	563	−34	73	597	546	−51	9
-	-	-	-	-	-	-	547	518	−79	62	541	494	−103	101
447	437	130	415	408	−29	132	420	413	−24	129	420	417	−20	103
	H_2S													
2780	2682	0	-	-	-	-	2765	2666	−16	1	2763	2665	−17	2
2755	2658	0	-	-	-	-	2425	2276	−382	440	2443	2292	−366	349
1193	1166	0	-	-	-	-	1215	1172	6	3	1220	1172	6	5
	H_2O			α-SO				α-SS				β-SS		
3938	3747	67	3887	3691	−56	75	-	-	-	-	-	-	-	-
3803	3622	4	3585	3387	−235	367	-	-	-	-	-	-	-	-
1622	1575	67	1642	1584	9	1868	-	-	-	-	-	-	-	-
	HXeSH													
2724	2634	7	2724	2628	−6	5	2721	2626	−8	5	2721	2626	−8	5
1450	1375	2800	1621	1488	113	3043	1573	1436	61	2317	1573	1436	61	2322
640	818	6	629	601	−25	12	632	601	−25	3	632	605	−21	2
538	630	0	530	512	−12	2	535	509	−15	0	535	508	−16	0
459	597	3	446	442	−18	2	447	443	−17	1	448	443	−17	1
253	248	43	247	242	−6	49	248	243	−5	53	248	240	−8	255
	H_2S													
2780	2682	0	-	-	-	-	2764	2664	−18	1	2764	2664	−18	1
2755	2658	0	-	-	-	-	2580	2482	−176	267	2580	2482	−176	267
1193	1166	0	-	-	-	-	1203	1167	1	4	1204	1169	3	4

[1] The value is calculated as $\Delta\nu_{anh} = \nu_{anh}(\text{complex}) - \nu_{anh}(\text{monomer})$.

The most intense band in computed α-OO spectrum is the Xe–H stretching mode at 1812 cm^{-1}, which is blue-shifted by 90 cm^{-1} compared to the monomer. The computed vibrational shift is in good agreement with the experimentally observed shift of +103 cm^{-1} [25]. According to the calculations, there are three notable vibrational modes red-shifted from the monomer to facilitate further the experimental assignment of this complex. These modes are computed to be at 3600 (OH stretch), 732 (HXeOH asym bend) and 408 cm^{-1} (Xe–OH stretch) and assignment is done according to Lundell et al. [45].

For the α-SO complex, the vibrational perturbations upon complexation with water molecule induce similar changes on HXeSH as it did with HXeOH. The most notable vibrational mode in the computed spectrum is the intense Xe–H stretching mode at 1488 cm^{-1}. This mode is blue-shifted +113 cm^{-1} compared with the isolated molecule, a shift equally large as found in the case of HXeOH. All the other modes of HXeSH are red-shifted upon complexation. The other bands are, however, quite weak according to computations and present a challenge for experimental detection. The Xe–SH stretching mode is at 242 cm^{-1}, and, even though it has a reasonable computed intensity, its position makes it to escape standard IR measurements.

All the noble-gas complexes with H_2S follow the trends set by the water complexes. In all computed complex structures, the Xe–H stretching mode is significantly intense and blue-shifted in analog of the water complexes. This also follows the reports of previous studies of complexes involving noble-gas molecules, where the Xe–H stretching mode is very sensitive to complexation and it is always found to be blue-shifted [12].

Based on the computations, the HXeOH-H_2S complexes could be identified experimentally since the HXeOH subunit appears to present many distinct vibrational modes that become significantly more intense upon complexation. On the other hand, even though HXeSH follows the trends set by HXeOH in H_2S complexes, the computations indicate smaller vibrational shifts and less intensity changes than in the corresponding HXeOH-H_2S complexes. The most plausible vibrational bands to identify HXeSH-H_2S complexes experimentally are the Xe–H stretching mode in HXeSH subunit and the vibrational modes of the H_2S subunit.

3.3. Supermolecular Interaction Analysis

The strength of the intermolecular interactions in the stable complex structures introduced above may be analyzed based on the values collected in Table 3, visualized also in Figure 2, which have been obtained within the supermolecular approach. The presented energy values are all BSSE-corrected and the zero-point harmonic vibrational energy correction calculated at MP2/aug-cc-pVDZ level is given separately.

Table 3. Supermolecular interaction energies calculated with various methods and zero-point energy (ZPE) correction using the aug-cc-pVDZ(-PP) basis set and harmonic approximation.

Energy	α-OO	γ-OO	α-OS	β-OS	γ-OS	ε-OS	α-SO	γ-SO	α-SS	β-SS	γ-SS	ε-SS
E_{int}^{HF}	−33.47	−7.16	−13.38	−12.80	0.27	8.55	−20.55	−9.06	−3.64	−3.38	0.52	11.99
E_{int}^{MP2}	−41.70	−8.68	−27.58	−27.13	−5.68	−0.37	−31.37	−9.10	−19.45	−19.30	−6.34	−1.52
E_{int}^{CCSD}	−40.20	−7.95	−22.06	−22.06	−3.50	1.78	−27.69	−7.11	−13.52	−13.36	−2.02	2.43
$E_{int}^{CCSD(T)}$	−40.96	−7.85	−23.91	−23.91	−4.19	0.03	−28.73	−6.59	−15.36	15.21	−2.60	−0.13
E_{int}^{MP4}	−39.69	−7.38	−2477	−24.40	−4.38	−0.90	−29.43	−7.04	−16.47	−16.35	−3.75	1.41
E_{ZPV}^{MP2}	9.66	2.99	6.08	5.99	2.76	1.86	8.45	3.41	5.30	5.38	3.13	2.78

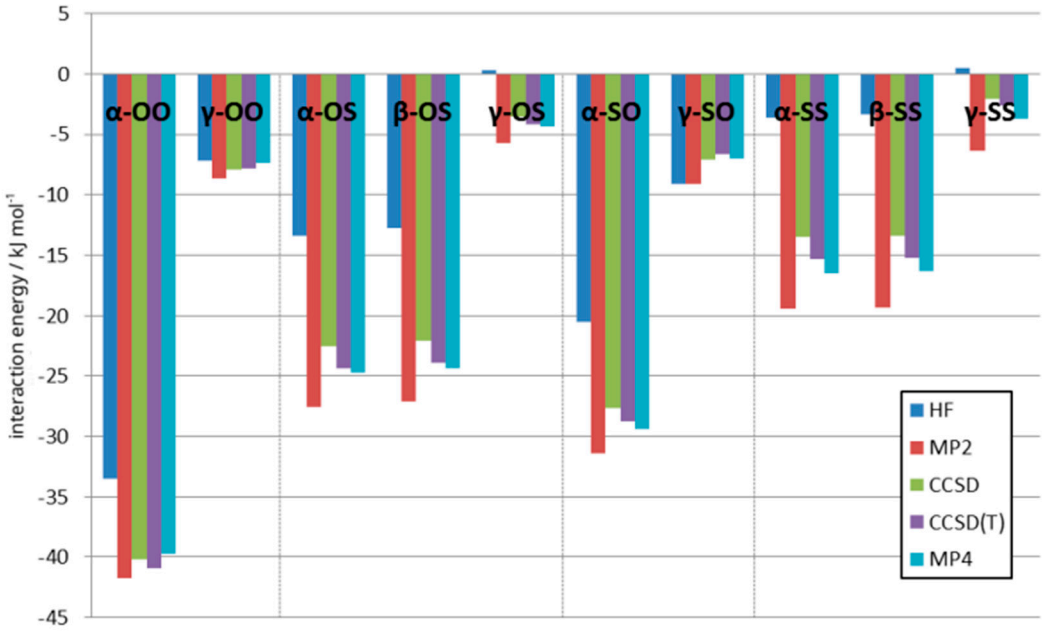

Figure 2. Bar graph illustrating the supermolecular interaction energies of the studied complexes obtained at different levels of theory. The energy values are given in kJ·mol^{-1}.

In all cases, the α form is found to be the most stable (if β form is present, it appears to be of almost same energy). The γ-form interaction energies are found to be much weaker and, especially in the complexes with H_2S, demonstrate very strong dependence on the correlation energy effects: these forms appear to be unstable at the pure Hartree-Fock level. On the other hand, when the correlation-effects are included, the particular level of the employed theory does not seem to be of high relevance in qualitative or quantitative analysis: one may only observe gentle, though systematic overestimation of the MP2 interaction energy with respect to the higher level methods.

Inclusion of an additional set of basis functions centered in the middle of the intermolecular hydrogen bonding results in the enhancement of interaction energies, as shown in Figure 3. The strongest stabilization effect is again found for the H_2S-containing γ-structures, further highlighting the important role of the electron correlation. In this case, one also observes the need for the inclusion of higher-order correlation effects, as MP2 method tends to overestimate the bonding energy stabilization when compared to the CCSD, CCSD(T), and MP4 approaches. The observed ghost-atom-induced stabilization can be interpreted as a sign of strong polarization effects modifying the electronic clouds of the monomers in the direction of the formed hydrogen bond. It also shows that such effects are especially important when the S atom in the H_2S monomer acts as the proton acceptor upon the hydrogen bonding formation; the analogous effect is much weaker for the less polarizable O-atom.

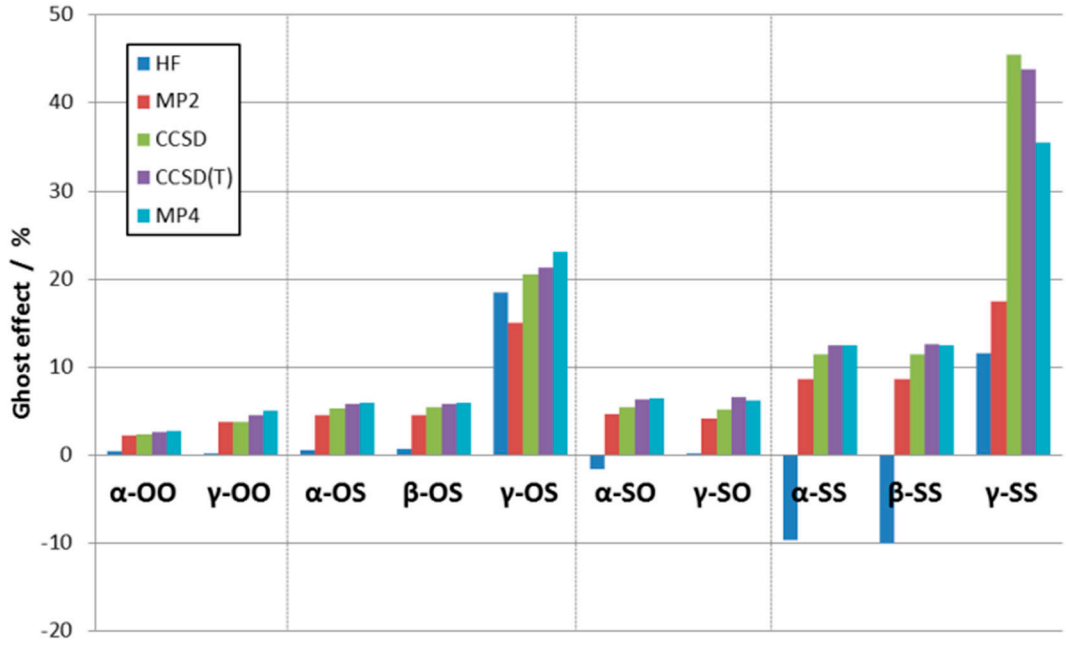

Figure 3. Bar graph illustrating the percentage effect of the placement of the mid-bond ghost atom on the supermolecular interaction energy.

From a chemical perspective, it turns out that the HXeOH and HXeSH complexes with H_2O are more stable than the ones with H_2S, even the HXeSH complex with water. Further analysis of the interaction energy decomposition within the symmetry-adapted perturbation approach may shed more light on this subject.

3.4. Decomposition of the Interaction Energy

Following the methodological scheme introduced in Section 2.3, SAPT interaction energy components have been computed for all the studied binary structures. They are presented in Table 4. A look at the obtained total interaction energies shows that they are in good qualitative agreement with the results obtained with the supermolecular method. As mentioned earlier, we refrained from the use of the $\delta E^{HF}_{int,resp}$ term. The reason is that it renders the SAPT results systematically overestimating the strength of the interaction compared to the supermolecular results. The term is especially large for α-OO, α-OS and β-OS, the systems in which the H_2O or H_2S molecules are neighboring the largely ionic $(HO)^-$–$(XeH)^+$ bonding. One could expect smaller induction effects in these three complexes since the HXeOH molecule has smaller dipole moment than HXeSH but it is not the case. We think that this discrepancy might be due to the inadequacy of the Hartree-Fock energy values for these systems. Even though the constituent molecules are polar and the use of the term is advised in such cases, here, the presence of xenon atom may cause unphysical terms to have substantial contribution to the energy [46]. Thus, we do not include the $\delta E^{HF}_{int,resp}$ term in further considerations.

Similar to the supermolecular case, with the SAPT method, the effect of addition of extra mid-bond functions on the interaction energy has been studied. However, the results, presented in Table S2 in Supplementary Materials, show systematic interaction enhancement of ca. 1 $kJ \cdot mol^{-1}$ for all the investigated structures. Thus, for the used SAPT approach, the chosen aug-cc-pVDZ(-PP) basis set may be considered satisfactorily saturated.

Again, one finds the α-OO form to be the most stable and the energy description furnished by SAPT is both qualitatively and quantitatively similar to the previously performed [27]. The forms α-SO, α-OS and β-OS show weaker interaction. The dihydrogen bonded structures are unstable at this level of SAPT. The inclusion of midbond functions decreased their energy but it remained positive. β structures have similar interaction energy as their α counterparts. Moving to the energy

decomposition analysis, presented as the fraction contributions to the total interaction energy in the bottom of Table 4, for all the minima, one observes a dominant role of the electrostatic attraction and repulsive Pauli-exchange interaction.

Interestingly, only in the α-OO, γ-OO and α-SO structures the E_{elst} term exceeds the E_{exch} repulsion, making these complexes stable at the first order perturbation theory level. In all other cases, the second order terms including induction and dispersion contributions are needed to explain the complex stability. The largest absolute induction energy values are noted for the systems in which the noble gas molecule is the proton acceptor. Overall, the complexes with water have visibly smaller induction contribution to the total interaction energy. An especially pronounced role of induction is observed for the γ-SS form.

The absolute dispersion energy is the largest for the α and β structures in which the O/S atom of the H_2O/S molecule is neighboring the noble gas atom of the other molecule creating a significant intermolecular contact. The complexes with sulfur atom in any of the constituent molecules show significantly larger relative dispersion contribution to the total interaction energy, especially the complexes with H_2S. The γ and ε structures have particularly large negative dispersion contribution while the total first order energy is positive. This explains why neither the γ nor the ε structures are stable at HF level. The ε structures are not stable at SAPT level but perhaps the higher order induction and dispersion terms would decrease the total interaction energy. Further calculations are needed. For a given composition, the complexes in which the noble gas molecule is the proton acceptor, i.e. α and β, have smaller dispersion contribution relative do the induction contribution (i.e., the fraction E_{disp}/E_{ind}) compared to the complexes where the noble gas molecule is the proton donor or is involved in DHB, i.e. γ and ε structural configurations.

It appears that only the systems including H_2S molecule are able to form the ε structures. Even though their total SAPT energies are positive, they are predicted to have negative supermolecular interaction energies. The SAPT results and the Mulliken charges analysis in Table 2 highlight the role of the induction and dispersion in these structures showing that, perhaps, only the larger polarizable clouds of sulfur atom allow for this type of interaction to take place. The larger absolute induction contribution also confirms the observed increase in charge separation and the decrease of intermolecular distance for the SS structure.

The relative contribution of the exchange energy to the total interaction energy is typically at least twice as much in the complexes with H_2S compared to the complexes with water. Because the other contributions do not increase as much this seems to be the reason for the stability of the complexes with water.

Table 4. The SAPT analysis of the intermolecular interaction energy in kJ·mol^{-1}.

Energy	α-OO	γ-OO	α-OS	β-OS	γ-OS	ε-OS	α-SO	γ-SO	α-SS	β-SS	γ-SS	ε-SS
E_{int}^{HF}	−33.47	−7.16	−13.38	−12.80	0.27	8.55	−20.55	−9.06	−3.64	−3.38	0.52	11.99
$E_{elst}^{(10)}$	−82.44	−17.98	−59.17	−57.11	−11.91	2.20	−54.07	−23.54	−35.75	−35.46	−17.98	0.43
$E_{exch}^{(10)}$	77.27	17.30	73.22	70.84	18.21	10.53	50.92	24.70	46.22	46.11	30.09	20.41
$E_{ind}^{(20)}$	−42.14	−8.39	−41.36	−40.56	−9.48	−4.29	−32.94	−14.06	−32.91	−33.02	−19.75	−9.80
$E_{ind-exch}^{(20)}$	23.87	5.10	25.55	24.99	7.00	2.37	21.89	9.41	24.16	24.26	15.60	6.35
$E_{disp}^{(20)}$	−27.13	−9.18	−28.11	−27.66	−10.85	−8.20	−22.48	−11.68	−23.20	−23.24	−15.31	−12.53
$E_{disp-exch}^{(20)}$	5.76	1.72	6.13	5.99	1.85	0.90	4.44	2.50	4.43	4.44	2.97	1.67
$E_{tot}^{(10)}$	−5.17	−0.68	14.04	13.73	6.30	12.73	−3.15	1.16	10.47	10.65	12.11	20.84
$E_{tot}^{(20)}$	−39.63	−10.75	−37.78	−37.24	−11.49	−9.22	−29.10	−13.83	−27.51	−27.55	−16.49	−14.31
$\delta E_{int,resp}^{HF}$	−10.04	−3.20	−11.61	−10.96	−3.55	−2.27	−6.34	−5.57	−5.36	−5.27	−7.44	−5.40
E_{int}^{SAPT}	−44.80	−11.43	−23.74	−23.51	−5.19	3.52	−32.25	−12.68	−17.05	−16.90	−4.38	6.53
E_{elst}/E_{int}^{SAPT}	1.84	1.57	2.49	2.43	2.29	0.62	1.68	1.86	2.10	2.10	4.11	0.07
E_{exch}/E_{int}^{SAPT}	−1.72	−1.51	−3.08	−3.01	−3.51	2.99	−1.58	−1.95	−2.71	−2.73	−6.87	3.13
E_{ind}/E_{int}^{SAPT}	0.41	0.29	0.67	0.66	0.48	−0.55	0.34	0.37	0.51	0.52	0.95	−0.53
E_{disp}/E_{int}^{SAPT}	0.48	0.65	0.93	0.92	1.73	−2.07	0.56	0.72	1.10	1.11	2.82	−1.66

4. Conclusions

In this paper we have reported the computationally investigated structures, vibrational spectra and intermolecular interaction energies using the supermolecular and SAPT approaches for HXeOH/SH···H_2O/S complexes. The calculations performed at various ab initio levels predict two structures for the complexes with H_2O and four structures for the complexes with H_2S. In the case of the complexes with H_2O, the α and γ structures are analogous to the structures found previously for HXeOH···H_2O; however, the δ structure was not confirmed in this study. In the case of the complexes with H_2S, we found similar structures (α and γ) together with two additional configurations (β and ε) where β is a cis-like variation of the α form and ε is dihydrogen-bonded structure.

The predicted Xe–H stretching modes for all the studied complexes show significant blue shifts upon complexion ranging from +113 to +59 cm^{-1}. This confirms the previous results for α-OO and shows the other structures follow the trend. The computational spectra show distinct characteristics which should allow for their experimental identification. Additionally, we found large shifts of the stretching modes of the complexed H_2O and H_2S molecules, which have not been reported in the experiment.

From the point of view of the energetics, considering a given composition of the complex, the α and β structures are the most stable and considering all the complexes, the ones with H_2O are more stable than the ones with H_2S. This can be explained with the exchange contribution to the total interaction energy being significantly larger for the complexes with H_2S compared to the complexes with H_2O while all the other terms do not undergo such a systematic change. The SAPT analysis also shows that the complexes involving sulfur atom tend to have larger relative dispersion contribution.

Supplementary Materials: The following are available online at http://www.mdpi.com/2304-6740/6/3/100/s1, Figure S1: Supermolecular energies with ghost atoms; Figure S2: Bar graph illustrating the supermolecular and SAPT interaction energies of the studied complexes; Figure S3: Bar graph illustrating the supermolecular and SAPT interaction energies of the studied complexes with midbond functions; Figure S4: Transition states between various complex conformers; Table S1: Supermolecular interaction energies calculated with various methods and zero-point energy correction using the aug-cc-pVDZ(-PP) basis set with midbond functions placed between the closest interacting atoms; Table S2: The SAPT analysis of the intermolecular interaction energy with the midbond functions in kJ/mol; Table S3: The anharmonic wavenumbers (cm^{-1}) and integrated intensities ($km \cdot mol^{-1}$) of infrared spectra of the complexes of HXeOH calculated using MP2/aug-cc-pVDZ(-PP) method. Zeros in this table mean negative anharmonic values which were positive within harmonic approximation; Table S4: The anharmonic wavenumbers (cm^{-1}) and integrated intensities ($km \cdot mol^{-1}$) of infrared spectra of the complexes of HXeSH calculated using MP2/aug-cc-pVDZ(-PP) method. Zeros in this table mean negative anharmonic values which were positive within harmonic approximation; Tables S5–S22: The coordinates of atoms in α-OO, γ-OO, α-OS, β-OS, γ-OS, ε-OS, α-SO, γ-SO, α-SS, β-SS, γ-SS, ε-SS, $TS_{\alpha\beta}$, $TS_{\beta\alpha}$, $TS_{\gamma\gamma}$ (OS), $TS_{\varepsilon\varepsilon}$ (OS), $TS_{\gamma\gamma}$ (SS), $TS_{\varepsilon\varepsilon}$ (SS) given in Å.

Author Contributions: Conceptualization, J.C. and J.L.; Methodology, J.J. and J.C.; Software, J.C., G.S. and J.J.; Formal Analysis, J.C., G.S and J.J.; Investigation, G.S., J.J. and J.C; Resources, J.C; Writing—Original Draft Preparation, J.C. and J.L.; Writing—Review and Editing, J.C. and J.L.; Visualization, J.C.; Supervision, J.C.; Project Administration, J.C.; and Funding Acquisition, J.C. and J.L.

Funding: This work was funded by the National Science Centre (Poland) grant No. 2011/03/D/ST4/01341 and the Interdisciplinary Centre for Mathematical and Computational Modeling of the University of Warsaw grant No. G56–12.

Acknowledgments: J.L. gratefully acknowledges the University of Jyvaskyla sabbatical grant system that made this work possible during research visits to the Department of Chemistry, University of Warsaw, Poland.

Conflicts of Interest: The authors declare no conflict of interest.

References

1. Pimentel, G.C.; McLellan, A.L. *The Hydrogen Bond*; W. H. Freeman and Company: Berkeley, CA, USA, 1960.
2. Desiraju, G.R.; Steiner, T. *The Weak Hydrogen Bond in Structural Chemistry and Biology*; Oxford University Press: Oxford, NY, USA, 1999; ISBN 0198502524.
3. Klemperer, W.; Vaida, V. Molecular complexes in close and far away. *Proc. Natl. Acad. Sci. USA* **2006**, *103*, 10584–10588. [CrossRef] [PubMed]

4. Vigasin, A.A.; Slanina, Z. *Molecular Complexes in Earth's, Planetary, Cometary and Interstellar Atmospheres*; World Scientific Publising Co. Inc.: Singapore, 1998; ISBN 981023211X.
5. Vaida, V. Perspective: Water cluster mediated atmospheric chemistry. *J. Chem. Phys.* **2011**, *135*, 020901. [CrossRef] [PubMed]
6. Sanloup, C.; Bonev, S.A.; Hochlaf, M.; Maynard-Casely, H.E. Reactivity of xenon with ice at planetary conditions. *Phys. Rev. Lett.* **2013**, *110*, 265501. [CrossRef] [PubMed]
7. Pettersson, M.; Khriachtchev, L.; Lundell, J.; Räsänen, M. A chemical compound formed from water and xenon: HXeOH. *J. Am. Chem. Soc.* **1999**, *121*, 11904–11905. [CrossRef]
8. Khriachtchev, L.; Isokoski, K.; Cohen, A.; Räsänen, M.; Gerber, R.B. A small neutral molecule with two noble-gas atoms: HXeOXeH. *J. Am.Chem. Soc.* **2008**, *130*, 6114–6116. [CrossRef] [PubMed]
9. Pettersson, M.; Lundell, J.; Räsänen, M. New rare-gas-containing neutral molecules. *Eur. J. Inorg. Chem.* **1999**, 729–737. [CrossRef]
10. Gerber, R.B. Formation of novel rare-gas molecules in low temperature matrices. *Ann. Rev. Phys. Chem.* **2004**, *55*, 55–78. [CrossRef] [PubMed]
11. Grochala, W.; Khriachtchev, L.; Räsänen, M. Noble Gas Chemistry. In *Physics and Chemistry at Low Temperatures*; Khriachtchev, L., Ed.; Pan Stanford Publishing: Singapore, 2011; Chapter 13; pp. 421–448.
12. Lignell, A.; Khriachtchev, L. Intermolecular interactions involving noble-gas hydrides: Where the blue shift of vibrational frequency is a normal effect. *J. Mol. Struct.* **2008**, *889*, 1–11. [CrossRef]
13. Lignell, A.; Lundell, J.; Khriachtchev, L.; Räsänen, M. Experimental and computational study of HXeY-HX complexes (X, Y = Cl and Br): An example of exceptionally large complexation effect. *J. Phys. Chem. A* **2008**, *112*, 5486–5494. [CrossRef] [PubMed]
14. Khriachtchev, L.; Tapio, S.; Räsänen, M.; Domanskaya, A.; Lignell, A. $HY\cdots N_2$ and $HXeY\cdots N_2$ complexes in solid xenon (Y = Cl and Br): Unexpected suppression of the complex formation for deposition at higher temperature. *J. Chem. Phys.* **2010**, *133*, 084309. [CrossRef] [PubMed]
15. Domanskaya, A.; Kobzarenko, A.V.; Tsivion, E.; Khriachtchev, L.; Feldman, V.I.; Gerber, R.B.; Räsänen, M. Matrix-isolation and ab initio study of HXeCCH complexed with acetylene. *Chem. Phys. Lett.* **2009**, *481*, 83–87. [CrossRef]
16. Yen, S.-Y.; Mou, C.-H.; Hu, W.-P. Strong hydrogen bonding between neutral noble-gas molecules (HNgF, Ng = Ar, Kr, and Xe) and hydrogen fluoride: A theoretical study. *Chem. Phys. Lett.* **2004**, *383*, 606–611. [CrossRef]
17. Jankowska, J.; Sadlej, J. Spectroscopic parameters in noble gas molecule: HXeF and its complex with HF. *Chem. Phys. Lett.* **2011**, *517*, 155–161. [CrossRef]
18. Esrafili, M.D. A theoretical investigation of the characteristics of hydrogen/halogen bonding interaction in dibromonitroaniline. *J. Mol. Mod.* **2013**, *19*, 1417–1427. [CrossRef] [PubMed]
19. Ma, L.; Huang, Z.; Niu, X.; Shen, T.; Guo, L. A theoretical study of the hydrogen bonding interactions in $HXeCCH\cdots Y$ (Y = H_2O and HF) complexes. *Comp. Theor. Chem.* **2013**, *1017*, 14–21. [CrossRef]
20. Mondal, S.; Chandra Singh, P. Noble gas indiced surprisingly higher stability of π hydrogen bonded complex: Comparative study of hydrogen bonded complexes of HKrCCH and HCCH with H_2O, NH_3, CH_3OH and CH_3NH_2. *RSC Adv.* **2014**, *4*, 20752–20760. [CrossRef]
21. Cohen, A.; Tsuge, M.; Khriachtchev, L.; Räsänen, M.; Gerber, R.B. Modeling of HXeBr in CO_2 and Xe environments: Structure, energetics and vibrational spectra. *Chem. Phys. Lett.* **2014**, *594*, 18–22. [CrossRef]
22. Esrafili, M.D.; Juyban, P.; Solimannejad, M. Exploring lithium bonding interactions between noble-gas hydrides HXeY and LiX molecules (Y = H, CN, NC and X = H, CN, NC, OH, NH_2, CH_3): A theoretical study. *Comp. Theor. Chem.* **2014**, *1027*, 84–90. [CrossRef]
23. Ryazantsev, S.V.; Lundell, J.; Feldman, V.I.; Khriachtchev, L. Photochemistry of the H_2O/CO system revisited: The $HXeOH\cdots CO$ complex in a xenon matrix. *J. Phys. Chem. A* **2018**, *122*, 159–166. [CrossRef] [PubMed]
24. Lundell, J.; Berski, S.; Latajka, Z. Dihydrogen-bonded complexes of xenon dihydride with water: Ab initio calculations and topological analysis of electron localisation function (ELF). *Phys. Chem. Chem. Phys.* **2000**, *2*, 5521–5527. [CrossRef]
25. Nemukhin, A.V.; Grigorenko, B.L.; Khriachtchev, L.; Tanskanen, H.; Pettersson, M.; Räsänen, M. Intermolecular complexes of HXeOH with water: Stabilization and destabilization effects. *J. Am. Chem. Soc.* **2002**, *124*, 10706–10711. [CrossRef] [PubMed]
26. Lundell, J.; Berski, S.; Lignell, A.; Latajka, Z. Quantum chemical study of the hydrogen-bonded $HXeOH\text{-}H_2O$ complex. *J. Mol. Struct.* **2006**, *790*, 31–39. [CrossRef]

27. Cukras, J.; Sadlej, J. Theoretical predictions of the spectroscopic parameters in noble-gas molecules: HXeOH and its complex with water. *Phys. Chem. Chem. Phys.* **2011**, *13*, 15455–15467. [CrossRef] [PubMed]
28. Tsivion, E.; Gerber, R.B. Lifetimes of compounds made of noble-gas atoms with water. *Chem. Phys. Lett.* **2009**, *482*, 30–33. [CrossRef]
29. Tsivion, E.; Räsänen, M.; Gerber, R.B. Destabilization of noble-gas hydrides by a water environment: Calculations for $HXeOH@(H_2O)_n$, $HXeOXeH@(H_2O)_n$, $HXeBr@(H_2O)_n$, $HXeCCH@(H_2O)_n$. *Phys. Chem. Chem. Phys.* **2013**, *15*, 12610–12616. [CrossRef] [PubMed]
30. Barone, V. Vibrational zero-point energies and theormodynamic functions beyond the harmonic approximation. *J. Chem. Phys.* **2004**, *120*, 3059–3065. [CrossRef] [PubMed]
31. Barone, V. Anharmonic vibrational properties by a fully automated second-order perturbative approach. *J. Chem. Phys.* **2005**, *122*, 014108. [CrossRef] [PubMed]
32. Frisch, M.J.; Trucks, G.W.; Schlegel, H.B.; Scuseria, G.E.; Robb, M.A.; Cheeseman, J.R.; Scalmani, G.; Barone, V.; Mennucci, B.; Petersson, G.A.; et al. *Gaussian09*; revision E.01; Gaussian Inc.: Wallingford, CT, USA, 2009.
33. Jeziorski, B.; Moszyński, R.; Szalewicz, K. Perturbation theory approach to intermolecular potential energy surfaces of van der Waals complexes. *Chem. Rev.* **1994**, *94*, 1887–1930. [CrossRef]
34. Jeziorska, M.; Jeziorski, B.; Čížek, J. Direct calculation of the Hartree-Fockinteraction energy via exchange-perturbation expansion. The He···He interaction. *Int. J. Quantum Chem.* **1987**, *32*, 149–164. [CrossRef]
35. Werner, H.-J.; Knowles, P.J.; Lindh, R.; Manby, F.R.; Schütz, M.; Celani, P.; Korona, T.; Mitrushenkov, A.; Rauhut, G.; Adler, T.B.; et al. *MOLPRO*, version 2009.1; A Package of ab Initio Programs. Available online: http://140.123.79.88/~silvercy/Data/Reference/quickstart.pdf (accessed on 13 September 2018).
36. Perez, F.; Granger, B.E. IPython: A system for interactive scientific computing. *Comput. Sci. Eng.* **2007**, *9*, 21–29. [CrossRef]
37. Jones, E.; Oliphant, T.; Peterson, P. SciPy: Open Source Scientific Tools for Python. 2001. Available online: www.scipy.org (accessed on 15 January 2018).
38. Hunter, J.D. Matplotlib: A 2D graphics environment. *Comput. Sci. Eng.* **2007**, *9*, 90–95. [CrossRef]
39. Cukras, J.; Sadlej, J. The influence of the dispersion corrections on the performance of DFT method in modeling HNgY noble gas molecules and their complexes. *Chem. Phys. Lett.* **2018**, *691*, 319–324. [CrossRef]
40. Lundell, J.; Pettersson, M. The dihydrogen-bonded complex $HXeH\text{-}H_2O$. *Phys. Chem. Chem. Phys.* **1999**, *1*, 1691–1697. [CrossRef]
41. Crabtree, R.H.; Siegbahn, P.E.M.; Eisenstein, O.; Rheingold, A.L.; Koetzle, T.F. A new intermolecular interaction: Unconventional hydrogen bonds with element-hydride bonds as proton acceptor. *Acc. Chem. Res.* **1996**, *29*, 348–354. [CrossRef] [PubMed]
42. Klooster, W.T.; Koetzle, T.F.; Siegbahn, P.E.M.; Richardson, T.B.; Crabtree, R.H. Study of the N–H···H–B dihydrogen bond including the crystal structure of BH_3NH_3 by neutron diffraction. *J. Am. Chem. Soc.* **1999**, *121*, 6337–6343. [CrossRef]
43. Bakhmutov, V.I. *Dihydrogen Bond: Principles, Experiments, and Applications*; John Wiley & Sons: Hoboken, NJ, USA, 2008; ISBN 978-0-470-18096-9.
44. Shimanouchi, T. *Tables of Molecular Vibrational Frequencies. Consolidated Volume I*; National Bureau of Standards: Gaithersburg, MD, USA, 1971; pp. 1–160. Available online: https://nvlpubs.nist.gov/nistpubs/Legacy/NSRDS/nbsnsrds6.pdf (accessed on 20 March 2018).
45. Lundell, J.; Chaban, G.M.; Gerber, R.B. Anharmonic vibrational spectroscopy calculations for novel rare-gas-containing compounds: HXeH, HXeCl, HXeBr, and HXeOH. *J. Phys. Chem. A* **2000**, *104*, 7944–7949. [CrossRef]
46. Patkowski, K.; Szalewicz, K.; Jeziorski, B. Orbital relaxation and the third-order induction energy in symmetry-adapted perturbation theory. *Theor. Chem. Acc.* **2010**, *127*, 211–221. [CrossRef]